


Levodopa-Induced Dyskinesia Are Mediated by Cortical Gamma Oscillations in Experimental Parkinsonism

Christopher Güttler, MD,¹ Jennifer Altschüler, MSc,¹ Kaloyan Tanev, MD,¹ Saskia Böckmann,¹ Jens Kersten Haumesser, MD,¹ Vadim V. Nikulin, PhD,² Andrea A. Kühn, MD,^{1,3,4} and Christoph van Riesen, MD^{1,3,4,5*} 

¹*Movement Disorder and Neuromodulation Unit, Department of Neurology, Charité University Medicine Berlin, Berlin, Germany*

²*Department of Neurology, Max Planck Institute for Human Cognitive and Brain Sciences, Leipzig, Germany*

³*Berlin Institute of Health, Berlin, Germany*

⁴*German Center for Neurodegenerative Diseases (DZNE), Bonn, Germany*

⁵*Department of Neurology, University Medical Center Göttingen, Göttingen, Germany*

ABSTRACT: Background: Levodopa is the most efficacious drug in the symptomatic therapy of motor symptoms in Parkinson's disease (PD); however, long-term treatment is often complicated by troublesome levodopa-induced dyskinesia (LID). Recent evidence suggests that LID might be related to increased cortical gamma oscillations.

Objective: The objective of this study was to test the hypothesis that cortical high-gamma network activity relates to LID in the 6-hydroxydopamine model and to identify new biomarkers for adaptive deep brain stimulation (DBS) therapy in PD.

Methods: We recorded and analyzed primary motor cortex (M1) electrocorticogram data and motor behavior in freely moving 6-OHDA lesioned rats before and during a daily treatment with levodopa for 3 weeks. The results were correlated with the abnormal involuntary movement score (AIMS) and used for generalized linear modeling (GLM).

Results: Levodopa reverted motor impairment, suppressed beta activity, and, with repeated administration, led to a

progressive enhancement of LID. Concurrently, we observed a highly significant stepwise amplitude increase in finely tuned gamma (FTG) activity and gamma centroid frequency. Whereas AIMS and FTG reached their maximum after the 4th injection and remained on a stable plateau thereafter, the centroid frequency of the FTG power continued to increase thereafter. Among the analyzed gamma activity parameters, the fraction of longest gamma bursts showed the strongest correlation with AIMS. Using a GLM, it was possible to accurately predict AIMS from cortical recordings.

Conclusions: FTG activity is tightly linked to LID and should be studied as a biomarker for adaptive DBS. © 2020 The Authors. *Movement Disorders* published by Wiley Periodicals LLC on behalf of International Parkinson and Movement Disorder Society

Key Words: gamma oscillations; dyskinesia; 6-OHDA

This is an open access article under the terms of the Creative Commons Attribution License, which permits use, distribution and reproduction in any medium, provided the original work is properly cited.

***Correspondence to:** Dr. Christoph van Riesen, Department of Neurology, University Medical Center Göttingen, Robert-Koch-Str. 40, 37075 Göttingen, Germany; E-mail: christoph.van-riesen@med.uni-goettingen.de

Relevant conflicts of interests/financial disclosures: The authors declare no conflict of interest.

Funding agencies: This study was funded by the German Research Council (grant number GE 2629/1-1 awarded to C.v.R.).

Received: 21 July 2020; **Revised:** 8 October 2020; **Accepted:** 30 October 2020

Published online in Wiley Online Library (wileyonlinelibrary.com). DOI: 10.1002/mds.28403

In Parkinson's disease (PD) a chronic progressive loss of dopaminergic neurons leads to the manifestation of debilitating motor symptoms in the form of akinesia, rigidity, and rest tremor. Recent cumulative evidence shows that the motor impairment is closely related to increased oscillatory neuronal network synchrony that can be recorded in the basal ganglia and motor cortex of PD patients and animal models of the disease.^{1,2} PD patients off dopaminergic medication show enhanced beta (13–35 Hz) oscillations that closely correlate with the severity of akinesia and rigidity.³ Furthermore, increased beta activity is greatly suppressed by known symptomatic treatments such as dopaminergic drugs (LD, dopamine receptor agonists) and deep brain

stimulation (DBS) of the subthalamic nucleus.⁴⁻⁷ Derived from these and other findings, it has been hypothesized that increased beta oscillations might mediate motor symptoms in PD.^{1,2} Currently, adaptive DBS devices that employ beta oscillations as a biomarker for akinesia are being developed and tested.^{8,9}

LD is the most efficacious drug in the symptomatic treatment of motor symptoms in PD.¹⁰ The long-term treatment with LD is often complicated by the occurrence of troublesome involuntary hyperkinesia, so-called “levodopa-induced dyskinesia” (LID), which severely affects the quality of life of patients.^{11,12} The main known risk factors for the development of LID are the severity and duration of the disease, as well as the dose and length of treatment with LD.¹²⁻¹⁵ Despite considerable advances in the pharmacotherapy of PD, it is notoriously difficult to suppress LID once it has started.¹⁶ The presence of disabling LID is a main reason for the initiation of DBS therapy.

How chronic LD medication leads to LID is a topic of ongoing research. A key mechanism in the pathogenesis of LID seems to be that the nonphysiological synthesis, release, and reuptake of dopamine metabolized from high-dose LD result in an aberrant synaptic plasticity at the cortico-striatal synapse.^{16,17} A subsequent increase in the activity of the movement promoting direct basal ganglia motor pathway is supposed to contribute to the generation of LID.¹⁶⁻¹⁸

Very little is known about the effect of chronic LD on network activity patterns in the brain over time and how these changes relate to LID. Only recently it has been shown in animal models of PD that repeated LD injections elicit enhanced narrow-band gamma oscillations, so-called “finely tuned gamma” (FTG), in motor cortex and striatum.^{19,20} A similar increase in gamma power was found in two PD patients with electrodes in the subthalamic nucleus and epidurally above the motor cortex.²¹ Because the recorded gamma levels were significantly higher for the motor cortex than for the studied subcortical regions, it was suggested that the motor cortex might have a primary role in the generation of LID.^{19,21}

Only recently, it has been repeatedly confirmed that oscillatory synchrony in neuronal networks is not a continuous signal but rather occurs as bursts of activity.²² In this regard, a growing amount of evidence from recordings of PD patients with implanted DBS electrodes ON and OFF levodopa suggests a close association between burst parameters at the beta frequency and the severity of the disease.^{23,24} It has been suggested that beta bursts might be superior biomarkers of movement symptoms in PD than average beta activity.²³⁻²⁵ The relevance of gamma bursts in LID had not yet been investigated.

Despite these recent advances in the understanding of the network pathophysiology underlying LID, many open questions remain. To further clarify the significance of cortical oscillations for the generation of LID,

we recorded electrocorticogram (ECoG) data from the primary motor cortex (M1) and assessed motor behavior in parkinsonian freely moving rats before and during a 3-week treatment with LD. Moreover, we further dissected network mechanism by testing the effect of different dopamine receptor antagonists on cortical signaling and dyskinesia. In conclusion, our findings provide compelling evidence for a close link between enhanced narrow-band cortical gamma oscillations and the priming and maintenance of LID.

Materials and Methods

Animals

All experimental procedures were performed on male Wistar rats (n = 10, 300–325 g, Harlan Winkelmann, Germany) in accordance with the European Union Directive 2010/63/EU as well as the German Animal Welfare Act (revised December 2018). Animals were kept on a 12-hour light cycle with ad libitum access to food and water. An overview of the experimental design of the study is shown in Figure 1A.

Surgical Procedures and Lesioning

Electrode implantations were performed 10 days after arrival. After induction and maintenance of isoflurane anesthesia, ophthalmic ointment was applied to prevent corneal dehydration. The animal was placed on a self-adjusting heating pad ($37 \pm 0.5^\circ\text{C}$) and transferred to a stereotaxic frame (David Kopf Instruments, Tujunga CA). The head was fixed in the flat-skull position using atraumatic ear-bars. After the scalp was incisioned along the midline, the epicranial aponeurosis was removed, and the skull was treated with dental bonding agent (OptiBond All-in-One, Kerr, Hanau FL). Dental composite (Charisma, Kulzer, Germany) was applied to the right-skull surface and cured with UV light (Translux Wave, Kulzer, Germany). Custom-made stainless-steel screw electrodes (M1, AP: +3, ML: +3; Ground, AP: -9, ML: ± 3), the custom-made guide cannula (MFB, AP: -2.6, ML: +1.6, DV: -6.4), and two silicon probes (DBC-2-3-A_ZIF16, Cambridge NeuroTech, UK, dorso-lateral striatum: AP: +0.6, ML: +3.6, DV: -4.5, and substantia nigra pars reticulata [SNpc]: AP: -5.2, ML: +2.4, DV: -8.2) were stereotactically implanted using the standard paxinos coordinate system²⁶ relative to bregma. Data from the silicon probes are not part of this publication. All connectors were attached to the electronic interface board (EIB2, Cambridge NeuroTech). All electronic parts were then covered in dental acrylic (Paladur, Kulzer, Germany). Animals were allowed to recover the following 3 days under close monitoring and daily pain medication (carprofen, 5 mg/kg subcutaneous).

Unilateral lesioning of midbrain dopaminergic neurons was carried out 17 days post-implantation. After

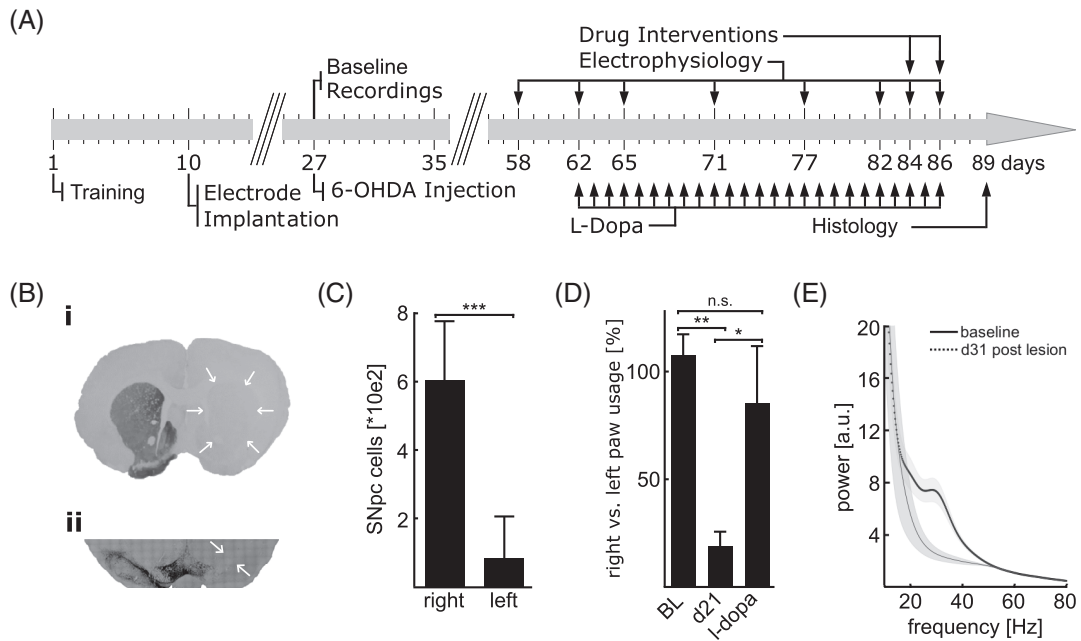


FIG. 1. (A) Experimental design. (B) Immunohistochemistry confirming loss of (i) striatal tyrosine hydroxylase (TH)-positive fibers and (ii) cell bodies in the substantia nigra pars compacta (SNpc). (C) Absolute count of TH+ SNpc cells (standard deviation [SD]). (D) Results of the cylinder test (SD). (E) Power spectral density of M1 ECoG (electrocorticogram) data.

isoflurane induction, a custom-made 33G steel cannula was carefully inserted into the guide cannula and lowered into the left medial forebrain bundle. Sterile-filtered 1 μ L of saline containing 8 μ g of 6-OHDA (Sigma-Aldrich Taufkirchen, Germany) was injected using a precision pump (Harvard apparatus Massachusetts, MA, USA).

Behavioral Testing

Unilateral motor impairment after dopaminergic lesioning was assessed using the cylinder test as previously reported.²⁷ Motor testing was performed before the injection of 6-OHDA on day 27 and thereafter on days 28, 41, 48, and 58 and 60 minutes after the first LD injection on day 62. The ratio of right- versus left-paw usage was analyzed using one-way analysis of variance with Bonferroni-corrected post hoc testing. Only animals with a sufficient dopaminergic deficit according to published criteria (contralateral paw usage <40% on day 21 post-lesion²⁸ and ipsilateral cell count of SNpc cells <20% of the contralateral side²⁹) and a complete data set (n = 5) were included in subsequent analyses. A pronounced dopaminergic lesion is known to be a prerequisite for the development of robust dyskinesia.^{28,29}

Initially all animals were extensively trained on the motorized treadmill (Bioseb, Pinellas Park, FL, USA) at increasing speeds up to 30 cm/s. For the recording sessions animals were placed on the treadmill before LD injection, and two sessions at 10 and 20 cm/s of 2 minutes each were recorded using an overhead camera at 10 frames/s coupled to the electrophysiological

recording setup. Periods of full compliance were identified and marked using a semiautomatic custom-written Matlab script (Mathworks Natick, MA, USA). This was followed by a 10-minute recording session at rest. Subsequently, after LD injection the 180-minute LID recording was started immediately. Exactly 15 minutes into the 180-minute recordings, the animals were transferred to the treadmill, recorded for 4 minutes (2 \times 2 minutes at 10 and 20 cm/s), and then returned to the recording cage for the remaining 160 minutes of the recordings. The electrophysiological data recorded between 15 and 20 minutes of the 180-minute recordings were excluded from the subsequent analysis on gamma oscillations.

The global abnormal involuntary movement score (AIMS) was calculated according to the published standard.³⁰ In brief, the animals were monitored for 1 minute every 20 minutes over an observation period of 3 hours immediately after L-dopa administration for signs of axial, limb, and orolingual dyskinesia. Persistency (basic score) and amplitude were scored for every observation period between 0 and 4 for every AIM subtype. The global AIMS was then calculated as

$$\text{Global AIM} = \sum_{i=1}^3 \text{persistency}_i \times \text{amplitude}_i.$$

Average AIMSs for the individual animals and recording sessions were calculated as the mean of the AIMSs rated 60, 80, 100, and 120 minutes after injections of LD.

Drug Treatments

All drugs were purchased from Sigma-Aldrich (St. Louis, MO), dissolved in isotonic saline, and administered subcutaneously. The animals received daily injections of 15 mg/kg L-dopa methyl ester and 8 mg/kg benserazide from days 62 to 86. On days 84 and 86, the D1 and D2 antagonists halobenzazepine (0.5 mg/kg) and raclopride (1 mg/kg) were injected s.c. 10 minutes before L-dopa.

Data Acquisition

Electrophysiological data were recorded using a wireless electrophysiological setup (W32, Triangle Bio-Systems, Durham, NC, USA) with the animals at rest and during treadmill exercise. Recordings were performed before lesioning and 1 month later (days 27 and 58), as well as before and immediately after the administration of L-dopa on days 62, 65, 71, 77, 82, 84, and 86. ECoG data were recorded at 30 kHz, amplified 800×, bandpass filtered (0.5–1000 Hz, 6th-order zero-phase butterworth filter), and resampled to 500 Hz with prior anti-aliasing finite impulse response low-pass filtering. Further analysis was performed using the Fieldtrip toolbox³¹ supplemented by custom-written Matlab code. Artifacts were identified using the fieldtrip automatic artifact rejection routine and custom-written Matlab scripts.

Power and Frequency

All recordings were converted to the spectral domain using continuous complex wavelet convolution with a time window of 6 cycles, 50% overlap, and hanning tapering (MTMCONV³¹). Power spectra were binned into 0 to 10/10 to 30/30 to 50/50 to 70/70 to 90/90 to 110/110 to 130/130 to 150/150 to 170, and 170 to 180 minutes after the injection of L-dopa and averaged. The resulting power spectra were then split into aperiodic and oscillatory components using the FOOOF toolbox.³² For FTG power analysis, the area under the curve (AUC) and the maximum amplitude of the oscillatory component between 70 and 140 Hz were calculated.

For frequency analysis the oscillatory dominant frequency (the power-weighted mean of the frequencies in a spectrum, ie, spectral centroid) was determined for the high-gamma frequency range, 50–130 minutes after L-dopa injection.

$$f_{\text{dominant}} = \frac{\sum_{i=70\text{ Hz}}^{140\text{ Hz}} \text{amplitude}_i \times i}{\sum_{j=70\text{ Hz}}^{140\text{ Hz}} \text{amplitude}_j}$$

The frequency shift was calculated as the absolute change in the dominant frequency compared to the

dominant frequency after the first L-dopa injection within each animal.

Burst Analysis

For burst detection the baseline recordings at rest immediately before and the 3-hour recordings after each L-dopa injection were bandpass filtered (10th-order zero-phase butterworth filter) with a passband frequency range of ± 5 Hz around the dominant high-gamma frequency of the 180-minute recording of the individual animal on that respective day (Supplementary Figure S1A). Next, the data were Hilbert transformed, and the envelope of the resulting analytical signal was extracted. The individual preinjection baseline recording was z-transformed $(X - \mu)/\delta$, and the 75th percentile of instantaneous power was identified as previously described by Tinkhauser et al.²⁴ The 3-hour post-L-dopa recording was z-transformed using mean and variance of the baseline recording. Bursts were identified as periods with instantaneous power continuously above the threshold and extracted for further analysis (Supplementary Figure S1C). Bursts occurring 50–130 minutes after L-dopa injection were included in subsequent histogram binning (burst power and length) as well as in average burst amplitude, length, and rate analysis.

Modeling

We first tested the applicability of only FTG power for detecting the presence of coinciding dyskinesia (AIMS > 0) by calculating the AUC of the receiver operating characteristic (ROC) curve with 95% bootstrap confidence intervals (nboot = 1000). We next performed a principal component analysis (PCA), including the previously identified burst parameters (percentage of the lowest and highest bins for burst amplitude, percentage of the shortest and longest bins for burst length, AUC of the power of the oscillatory component between 70 and 140 Hz, dominant frequency). The principal components with the highest eigenvalues were then selected until the combined amount of variance explained reached 95%. Generalized linear models with logistic regression were then fitted with the binary response variables AIMS > 0 or AIMS > 3 and evaluated with 10-fold cross-validation.

Histology

After the final recordings all animals received a lethal dose of urethane (3 g/kg) and were transcardially perfused with phosphate buffered saline and then with 4% paraformaldehyde. The brains were postfixed for 24 hours in 4% PFA, sucrose-cryoprotected, and frozen at -80°C until 40- μm coronal sectioning. Electrode trajectories were evaluated on Nissl-stained sections. The loss of dopaminergic SNpc cells was quantified using 3,3'-diaminobenzidin staining for tyrosine hydroxylase

(TH). Five sections spanning the anterior–posterior SNpc axis from each animal were incubated with a primary anti-TH mouse antibody (1:10,000, Sigma [T1299]) followed by a secondary biotinylated anti-mouse antibody (1:200, Vector BA-200, Vector Laboratories, Burlingame CA) and standardized avidin-biotin complex procedures. The sections were then mounted on glass slides, and images were obtained on a confocal microscope (Leica SPE, Leica Microsystems, Wetzlar Germany). Finally, the labeled SNpc cells on each section were counted manually. The ipsi- and contralateral TH+ SNpc cells were separately added up across the five sections spanning the SNpc.

The *P*-values of all statistical tests performed throughout the analysis are provided in Supplementary Table S1.

Results

In the present study, we investigated the association of M1 ECoG and motor performance in individual rats in 3 different states: after the implantation of the electrodes before the interventions, 35 days after a 6-OHDA lesion, and during 21 days of daily treatment with levodopa/benserazide (LD; Fig. 1A). Then, we studied the effect of a combined treatment of LD and the D1 and D2 receptor antagonists halobenzazepine and raclopride (Fig. 1A). After the completion of the initial recordings, a unilateral injection of 6-OHDA (8 μ g) into the MFB was performed, which induced a loss of TH-positive fibers in the striatum and a sub-maximal reduction in dopaminergic cells in the SNpc in comparison to the non-lesioned side (Fig. 1B,C). On a behavioral level, rats exhibited profound hemiakinesia contralateral to the lesion, which could be promptly reversed by the injection of LD (Fig. 1D).

Levodopa Suppresses Cortical Beta Power

In agreement with previous reports, in attentive resting animals we found a significant enhancement of beta oscillations in the M1 ECoG after the completion of the 6-OHDA lesion (day 31 post-lesion) in comparison with the recordings before the injection of 6-OHDA (Fig. 1E). A similar level of beta power could be shown in the recordings immediately before the LD injection with no significant change over time (Supplementary Figure S2A). On average, LD strongly suppressed beta activity (Off LD: 4.3 ± 0.9 AUC, On LD: 2.4 ± 0.9 AUC, $P < 0.001$; Supplementary Figure S2B), as previously shown by us and others.^{27,33}

Levodopa Leads to a Progressive Increase in AIMS

Thirty-one days after the 6-OHDA lesion, the animals were treated once daily with LD for 3 weeks. At days 1, 4, 10, 16, and 21, we recorded M1 ECoG as

well as videotaped motor behavior. The experimental sessions always commenced with a recording of 20 minutes at rest when LD was injected. Then, dyskinesia was rated using the abnormal involuntary movements scale (AIMS) every 20 minutes for 3 hours.³⁴ The well-described subcategories of axial, limb, and orolingual AIMS were assessed separately by two blinded video raters (K.T. and S.B.) offline. The global AIMS was calculated as published.²⁸

Whereas the first injection resulted in a minor increase in the global AIMS, the fourth and all later injections produced maximal dyskinesia. There was no significant difference in AIMS between the 2nd, 3rd, 4th, and 5th time points (Fig. 2Bi,C). When either the dopamine receptor antagonist halobenzazepine (D1) or raclopride (D2) was given before the LD treatment, the expression of AIM could be partly blocked (Fig. 2Bi,C).

Repeated Levodopa Injections Result in a Stepwise Increase in Cortical Gamma Power

All LD applications were followed by a striking increase in narrow-band high-gamma oscillations (FTG) with an average frequency of 97 Hz (range: 84–113 Hz) that was distinct from high-gamma power at rest and during movement (Fig. 2A; Supplementary Figure S3A). Already the 1st LD injection produced a pronounced increase in FTG activity (LD1: 3.1 ± 0.9 AUC; Fig. 2Bii,D). After the 4th injection, an additional significant enhancement could be noted (LD4: 9.9 ± 3.3 AUC; Fig. 2Bii,D). Then, FTG levels remained elevated (LD 10/16/21; Fig. 2Bii,D). There was no difference in the time interval between LD injection and maximal FTG power across all time points (Supplementary Figure S3B). During the individual recordings the centroid frequency of the gamma oscillations remained constant (data not shown). In contrast, across the recording days, a constant increase in the individual gamma centroid frequency could be observed (Fig. 2E). Despite the parallel increase in total FTG power and FTG frequency, there was a strong correlation neither between FTG power and frequency nor between FTG power and frequency shift (Supplementary Figure S3C). The application of raclopride and halobenzazepine before LD drastically reduced FTG power with a more-pronounced effect of halobenzazepine (Fig. 2D). Despite the reduction in the amplitude of the FTG due to the antagonist treatments, the centroid frequency continued to increase with the 22nd and 23rd LD injection (Fig. 2E).

Levodopa Increases the Duration and Amplitude of Gamma Bursts

To further specify the relation between gamma activity and LID, we calculated and sorted gamma bursts. Our analysis showed that across all investigated time

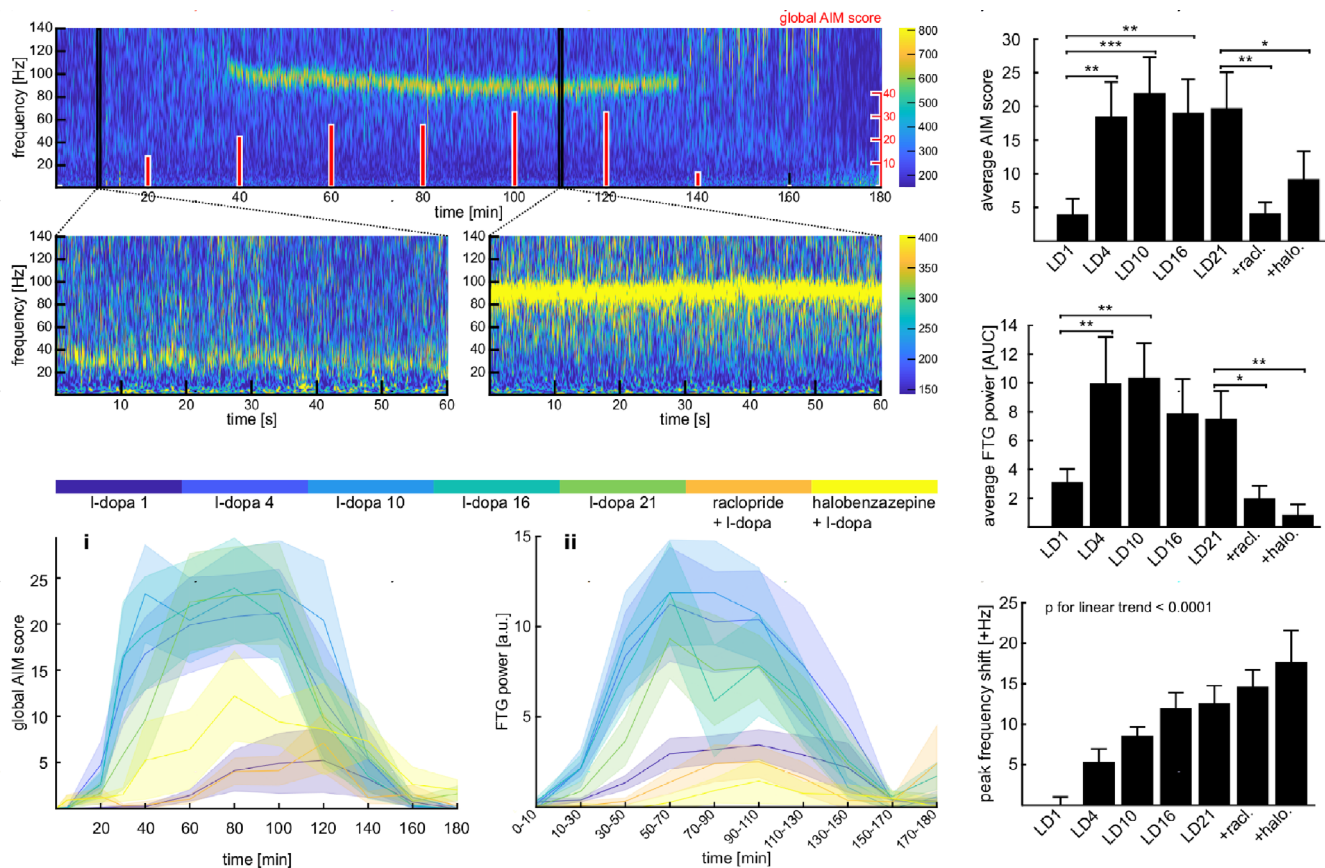


FIG. 2. Evolution of finely tuned gamma (FTG) oscillations in M1 ECoG (electrocorticogram) and dyskinesia in parkinsonian rats treated with LD for 21 days. **(A)** Exemplary time frequency spectrogram (18th injection of LD). Red bars: AIMS (abnormal involuntary movement score). Lower panels represent 60-second time segments before and during maximal dyskinesia. **(B)** Development of (i) average AIMS and (ii) average FTG power during 180 minutes after LD injections on different recording days. The x-axis depicts time after injection, successive injections are color coded (mean \pm standard error). **(C, D)** Average AIMS and FTG power AUC 50–130 minutes after LD injection. **(E)** Increase in FTG centroid frequency. [Color figure can be viewed at wileyonlinelibrary.com]

points, the rate, amplitude, and duration of gamma bursts increased ON LD in comparison to OFF LD (Fig. 3A). Whereas burst amplitude and duration were strongly correlated to the increase in FTG power over repeated injections of LD, burst rate showed the most pronounced increase after the 1st injection (Fig. 3B; Supplementary Figure S3D).

A further categorization of burst durations and amplitudes into defined bins revealed highly significant changes in the distribution of bursts for all time points (Fig. 3C,D). Whereas before LD injection short bursts with smaller amplitudes were more common, there was a clear shift toward longer bursts with higher amplitudes ON LD (Fig. 3C,D). Significant differences in burst amplitude could be noted for very short (50–100 ms) and very long (>200 ms) as well as for very low (z-scores 0–1) and very high-amplitude (z-scores > 3) bursts (Fig. 3C,D). Although the increase in the fraction of the longest and highest bursts after the injection of LD remained significant in comparison to the respective baselines over time, there was a

significant decrease in the fraction of highest bursts between the 4th and the 21st LD injections (Fig. 3C). The prior treatment with the dopamine receptor antagonists raclopride and halobenzazepine before the administration of LD suppressed the observed changes in mean burst amplitude and duration as well as in the distribution of burst amplitudes and burst duration ON and OFF LD (Fig. 3C,D).

Both FTG Power and Gamma Burst Parameters Correlate With AIMS

FTG power significantly correlated with the global AIMS ($\rho = 0.75$, $P < 0.001$; Fig. 4A). Spearman's ρ was similar across all investigated times, indicating that the correlation was not mainly driven by any particular time point (Supplementary Figure S3E). The analysis of categorized gamma bursts showed even stronger correlations. The occurrence of gamma bursts with very long durations strongly correlated with AIMS ($\rho = 0.80$, $P < 0.0001$; Fig. 4C), whereas the fraction of the

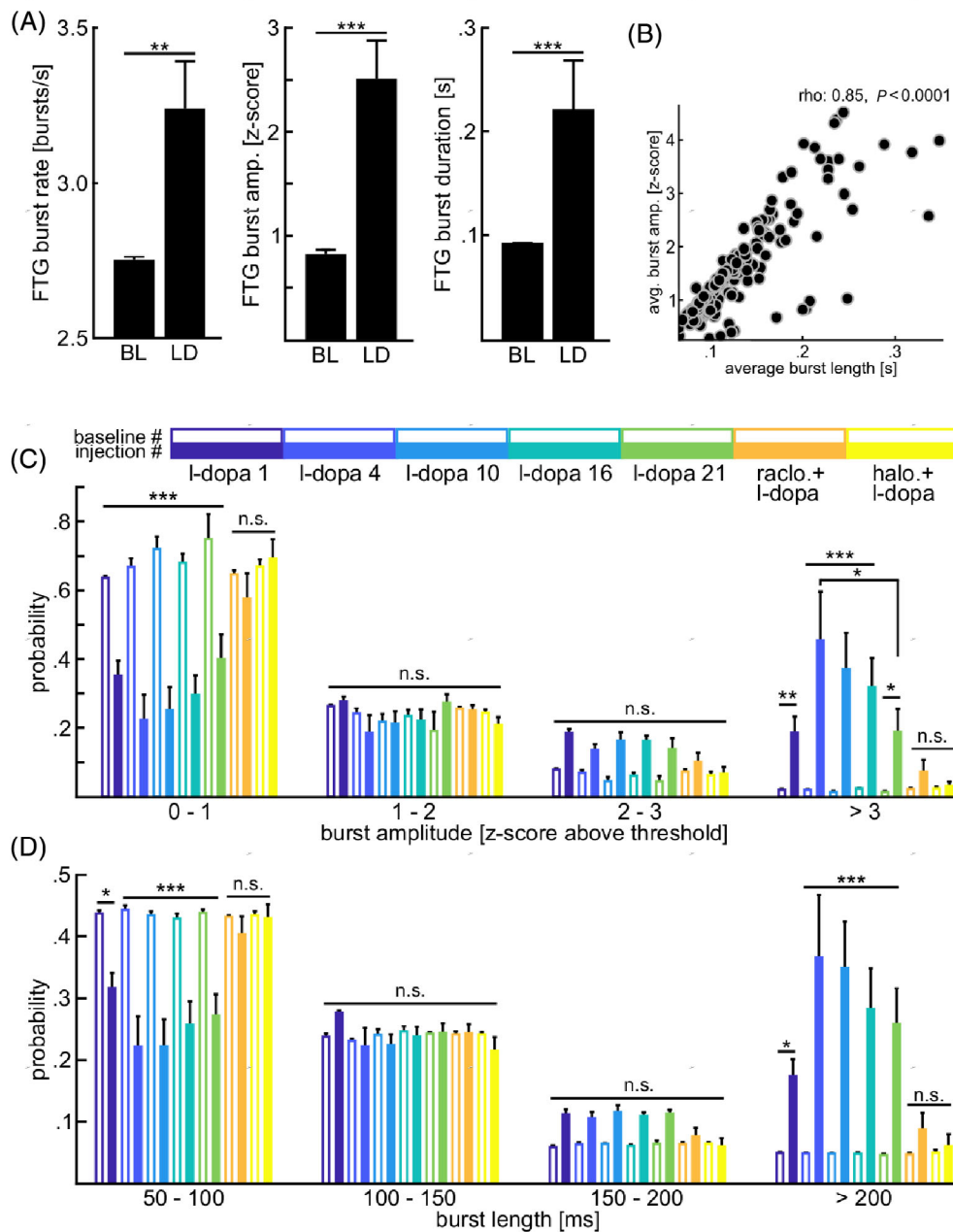


FIG. 3. Evolution of gamma burst parameters. **(A)** Average burst rate, amplitude, and duration. **(B)** Burst amplitude and burst length are highly correlated (spearman's rho). **(C, D)** Probability of binned burst amplitude and length (solid bars) compared to the respective baseline values (open bars) (standard error). [Color figure can be viewed at wileyonlinelibrary.com]

highest-amplitude bursts showed an intermediate correlation with AIMS ($\rho = 0.60$, $P < 0.0001$; Fig. 4B).

The FTG power spectral centroid frequency also moderately correlated with AIMS ($\rho = 0.54$, $P < 0.001$; Supplementary Figure S3F). FTG power and FTG frequency as well as FTG power and FTG frequency shift over time were not related. AIMS and FTG showed the weakest correlation when the animals were treated with a combination of LD

and halobenzazepine or raclopride (Supplementary Figure S3G).

Burst Parameters Outperform Power Thresholding for Detection of Dyskinetic States

To further emphasize the close relation between FTG and dyskinesia, we next tested whether we could reliably predict the levels of dyskinesia from ECoG

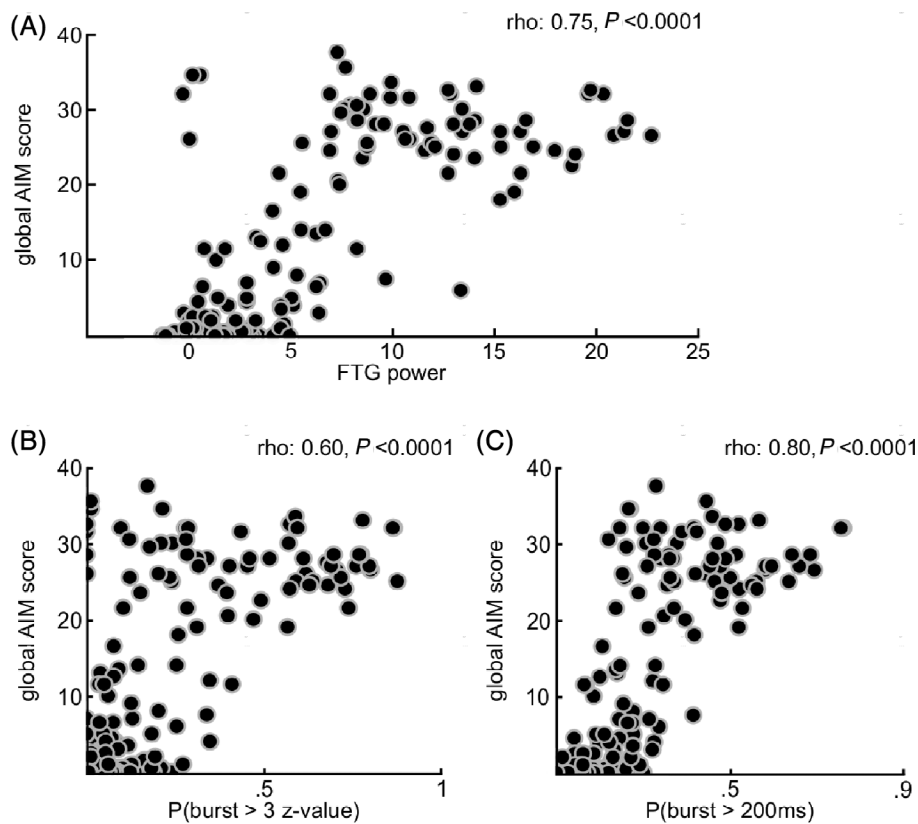


FIG. 4. Correlation of electrophysiological biomarkers and dyskinesia scores. **(A–C)** FTG (finely tuned gamma), the fraction of the longest and highest bursts correlates highly significantly with AIMS (abnormal involuntary movement score) (spearman's correlation, individual data points represent the binned recording intervals of the individual animals on days 62, 65, 71, 77, and 82).

recordings, which might be central for further developments of adaptive closed-loop DBS systems. We first tried to identify dyskinetic states ($AIM > 0$) with ECoG data using a simple FTG thresholding approach, which yielded a ROC-AUC of 0.86 (Fig. 5A). Because burst parameters proved to be more robustly correlated with the behavioral data, we chose to subject the latter to generalized linear modeling (GLM) with logistic regression after PCA dimensionality reduction (Fig. 5B, eigenvalues: PC1 4.49, PC2 1.04, and PC3 0.21). This procedure classified the behavioral states into whether dyskinesias are present or absent with an improved ROC-AUC of 0.89 by mainly increasing the specificity of the optimal operating point of the ROC curve (sensitivity 85%, specificity 82%; Fig. 5C). The sensitivity of the GLM versus power classifier at a false-positive rate of 0.1 for the $AIMS > 0$ case is 0.78 versus 0.68. Because mild dyskinesias may be non-bothersome and in some cases even sought after as a marker of sufficient therapy, we further tested the model using a cutoff of $AIMS > 3$, yielding a ROC-AUC of 0.97 with a high sensitivity of 94% and specificity of 92% (Fig. 5D).

Discussion

Enhanced high-gamma activity has been repeatedly shown in recordings from the basal ganglia and motor cortex of PD patients during LID and in animal models of the disease.^{19–21,33,35,36} The few publications that investigated an association between gamma activity and dyskinesia scores found variable correlations.^{19–21} We provide new evidence for a close relation of excessive cortical gamma activity recorded above M1 with the clinical severity of LID in the 6-OHDA model of PD. Although we found a high correlation of FTG power with AIMS, we could demonstrate an even higher relation with the height and length of gamma bursts. Using burst parameters in a generalized linear model, we could highly reliably predict the level of dyskinesia in our animals. By introducing gamma burst parameters from M1 into our model, we reach a classification performance comparable to previously published data, which relied on recordings from a multitude of different nodes in the cortico-basal ganglia thalamic loop.³⁷

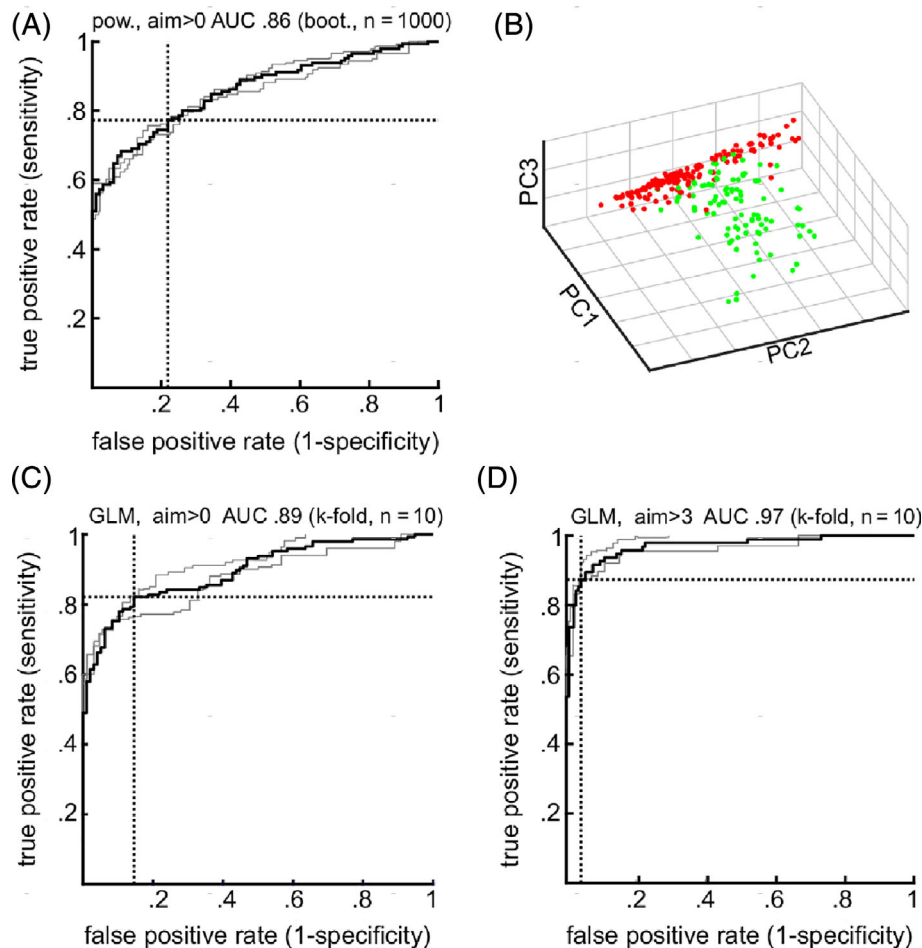


FIG. 5. Model performance measures. **(A)** Thresholding the M1 ECoG (electrocorticogram) FTG (finely tuned gamma) power for predicting the presence of any dyskinesia yields an AUC (area under the curve) of 0.86 (confidence intervals in gray, bootstrap $n = 1000$). **(B)** Separation of dyskinetic (green) versus non-dyskinetic (red) states according to the three selected principal components. **(C)** Generalized linear modeling with burst parameters increases the AUC to 0.89 (confidence intervals in gray, 10-fold cross-validation). Note the reduction in the false-positive rate. **(D)** Focusing on clinically significant dyskinesia with AIMS (abnormal involuntary movement score) >3 allows for almost-perfect classification (confidence bounds in gray, 10-fold cross-validation). [Color figure can be viewed at wileyonlinelibrary.com]

It has been hypothesized that the excessive gamma synchronization disturbs physiological network function in motor networks and thus leads to hyperkinetic movements. Despite this, FTG does not seem to be unique to dyskinesia in PD patients because it has also been shown in invasive recordings from patients suffering from dystonia and myoclonus epilepsy at rest.^{38,39} However, it has been assumed that FTG is distinct from the broadband low-amplitude increase in gamma oscillations that has been shown to accompany voluntary movement.^{40–42} In agreement with these previous publications, we found that dyskinesia and voluntary movement can be clearly differentiated by their gamma activity profile using M1 ECoG (Supplementary Figure S3A). This distinction is very important when considering using gamma oscillations as biomarkers to control neuromodulatory therapies.

Accumulating evidence shows that DBS-tailored electrophysiological biomarkers in real time (closed-loop

DBS [cl-DBS]) has the potential to outperform conventional continuous DBS regimes, which are currently used in standard clinical care.^{43–46} The development of cl-DBS was so far mainly focused on the detection of akinesia by assessing beta power in local field potentials from the subthalamic nucleus to trigger electrical stimulation in patients in their off-medication state.^{8,9,47} However, because most patients continue to take dopaminergic medication after the initiation of DBS therapy, there is also a need for the detection of dyskinesia from electrophysiological signals to stop or reduce stimulation to avoid a further exacerbation of drug-induced dyskinesia by DBS. In fact, only recently has it been demonstrated that chronic recordings of M1 ECoG are feasible and that they can be used to sense cortical gamma oscillations during LID in PD patients.^{48,49} Moreover, in a proof-of-principle study the level of cortical gamma power was used to modify the amplitude of STN DBS in an implanted closed-loop system.⁵⁰

Derived from our data, we propose that gamma burst parameters, especially the fraction of very high and long gamma bursts, should be further explored as possible biomarkers for LID in adaptive cl-DBS.

Author Roles

(1) Research project: A. Conception, B. Organization, C. Execution; (2) Statistical analysis: A. Design, B. Execution, C. Review and critique; (3) Manuscript preparation: A. Writing of the first draft, B. Review and critique.

C.G.: 1B, 1C, 2A, 2B, 3A

J.A.: 1C, 2C, 3B

K.T.: 1C, 2C, 3B

S.B.: 1C, 2C, 3B

J.K.H.: 1C, 2C, 3B

V.V.N.: 2A, 2B, 2C

A.A.K.: 1A, 1B, 2C, 3B

C.v.R.: 1A, 1B, 2A, 2B, 3A

Full financial disclosures for the previous 12 months

C.G., J.A., K.T., S.B., J.K.H., V.V.N., C.v.R.: none. A.A.K.: advisory board: Boston Scientific and Medtronic; Honoraria: Boston Scientific, Medtronic, and Abbott; lectures for Teva and Ipsen. ■

Acknowledgment: Open access funding enabled and organized by Projekt DEAL. ■

References

- Brown P. Abnormal oscillatory synchronisation in the motor system leads to impaired movement. *Curr Opin Neurobiol* 2007;17(6):656–664.
- Stein E, Bar-Gad I. Beta oscillations in the cortico-basal ganglia loop during parkinsonism. *Exp Neurol* 2013;245:52–59.
- Neumann WJ, Degen K, Schneider GH, et al. Subthalamic synchronized oscillatory activity correlates with motor impairment in patients with Parkinson's disease. *Mov Disord* 2016;31(11):1748–1751.
- Eusebio A, Thevathasan W, Doyle Gaynor L, et al. Deep brain stimulation can suppress pathological synchronisation in parkinsonian patients. *J Neurol Neurosurg Psychiatry* 2011;82(5):569–573.
- Kuhn AA, Kempf F, Brucke C, et al. High-frequency stimulation of the subthalamic nucleus suppresses oscillatory beta activity in patients with Parkinson's disease in parallel with improvement in motor performance. *J Neurosci* 2008;28(24):6165–6173.
- Kuhn AA, Kupsch A, Schneider GH, Brown P. Reduction in subthalamic 8-35 Hz oscillatory activity correlates with clinical improvement in Parkinson's disease. *Eur J Neurosci* 2006;23(7):1956–1960.
- Kuhn AA, Tsui A, Aziz T, et al. Pathological synchronisation in the subthalamic nucleus of patients with Parkinson's disease relates to both bradykinesia and rigidity. *Exp Neurol* 2009;215(2):380–387.
- Little S, Pogosyan A, Neal S, et al. Adaptive deep brain stimulation in advanced Parkinson disease. *Ann Neurol* 2013;74(3):449–457.
- Rosa M, Arlotti M, Ardolino G, et al. Adaptive deep brain stimulation in a freely moving parkinsonian patient. *Mov Disord* 2015;30(7):1003–1005.
- Connolly BS, Lang AE. Pharmacological treatment of Parkinson disease: a review. *JAMA* 2014;311(16):1670–1683.
- Hametner E, Seppi K, Poewe W. The clinical spectrum of levodopa-induced motor complications. *J Neurol* 2010;257(Suppl 2):S268–S275.
- Perez-Lloret S, Negre-Pages L, Damier P, et al. L-DOPA-induced dyskinesias, motor fluctuations and health-related quality of life: the COPARK survey. *Eur J Neurol* 2017;24(12):1532–1538.
- Fahn S, Oakes D, Shoulson I, et al. Levodopa and the progression of Parkinson's disease. *N Engl J Med* 2004;351(24):2498–2508.
- Schrag A, Quinn N. Dyskinesias and motor fluctuations in Parkinson's disease. A community-based study. *Brain* 2000;123(Pt 11):2297–2305.
- Stocchi F, Rascol O, Kiebertz K, et al. Initiating levodopa/carbidopa therapy with and without entacapone in early Parkinson disease: the STRIDE-PD study. *Ann Neurol* 2010;68(1):18–27.
- Bezard E, Brotchie JM, Gross CE. Pathophysiology of levodopa-induced dyskinesia: potential for new therapies. *Nat Rev Neurosci* 2001;2(8):577–588.
- Cenci MA, Jorntell H, Petersson P. On the neuronal circuitry mediating L-DOPA-induced dyskinesia. *J Neural Transm* 2018;125(8):1157–1169.
- Kishore A, Popa T. Cerebellum in levodopa-induced dyskinesias: the unusual suspect in the motor network. *Front Neurol* 2014;5:157.
- Dupre KB, Cruz AV, McCoy AJ, et al. Effects of L-dopa priming on cortical high beta and high gamma oscillatory activity in a rodent model of Parkinson's disease. *Neurobiol Dis* 2016;86:1–15.
- Halje P, Tamte M, Richter U, Mohammed M, Cenci MA, Petersson P. Levodopa-induced dyskinesia is strongly associated with resonant cortical oscillations. *J Neurosci* 2012;32(47):16541–16551.
- Swann NC, de Hemptinne C, Miodinovic S, et al. Gamma oscillations in the hyperkinetic state detected with chronic human brain recordings in Parkinson's disease. *J Neurosci* 2016;36(24):6445–6458.
- Feingold J, Gibson DJ, DePasquale B, Graybiel AM. Bursts of beta oscillation differentiate postperformance activity in the striatum and motor cortex of monkeys performing movement tasks. *Proc Natl Acad Sci U S A* 2015;112(44):13687–13692.
- Deffains M, Iskhakova L, Katabi S, Israel Z, Bergman H. Longer beta oscillatory episodes reliably identify pathological subthalamic activity in parkinsonism. *Mov Disord* 2018;33(10):1609–1618.
- Tinkhauser G, Pogosyan A, Tan H, Herz DM, Kuhn AA, Brown P. Beta burst dynamics in Parkinson's disease OFF and ON dopaminergic medication. *Brain* 2017;140(11):2968–2981.
- Lofredi R, Tan H, Neumann WJ, et al. Beta bursts during continuous movements accompany the velocity decrement in Parkinson's disease patients. *Neurobiol Dis* 2019;127:462–471.
- Paxinos G, Watson C. The rat brain in stereotaxic coordinates. 7th ed. Cambridge: Academic Press; 2013.
- Kuhn J, Haumesser JK, Beck MH, et al. Differential effects of levodopa and apomorphine on neuronal population oscillations in the cortico-basal ganglia loop circuit in vivo in experimental parkinsonism. *Exp Neurol* 2017;298:122–133.
- Cenci MA, Lundblad M. Ratings of L-DOPA-induced dyskinesia in the unilateral 6-OHDA lesion model of Parkinson's disease in rats and mice. *Curr Protoc Neurosci* 2007;41(1):9.25–25.23.
- Cenci MA. L-DOPA-induced dyskinesia: cellular mechanisms and approaches to treatment. *Parkinsonism Relat Disord* 2007;13(Suppl 3):S263–S267.
- Lundblad M, Andersson M, Winkler C, Kirik D, Wierup N, Cenci MA. Pharmacological validation of behavioural measures of akinesia and dyskinesia in a rat model of Parkinson's disease. *Eur J Neurosci* 2002;15(1):120–132.
- Oostenveld R, Fries P, Maris E, Schoffelen JM. FieldTrip: open source software for advanced analysis of MEG, EEG, and invasive

- electrophysiological data. *Comput Intell Neurosci* 2011;2011:156869.
32. Haller M, Donoghue T, Petersen E, et al. Parameterizing neural power spectra. *bioRxiv* 2018. <https://doi.org/10.1101/299859>
 33. Delaville C, McCoy AJ, Gerber CM, Cruz AV, Walters JR. Subthalamic nucleus activity in the awake hemiparkinsonian rat: relationships with motor and cognitive networks. *J Neurosci* 2015;35(17):6918–6930.
 34. Winkler C, Kirik D, Bjorklund A, Cenci MA. L-DOPA-induced dyskinesia in the intrastriatal 6-hydroxydopamine model of parkinson's disease: relation to motor and cellular parameters of nigrostriatal function. *Neurobiol Dis* 2002;10(2):165–186.
 35. Alegre M, Lopez-Azcarate J, Alonso-Frech F, et al. Subthalamic activity during diphasic dyskinesias in Parkinson's disease. *Mov Disord* 2012;27(9):1178–1181.
 36. Alonso-Frech F, Zamarbide I, Alegre M, et al. Slow oscillatory activity and levodopa-induced dyskinesias in Parkinson's disease. *Brain* 2006;129(Pt 7):1748–1757.
 37. Tamte M, Brys I, Richter U, Ivica N, Halje P, Petersson P. Systems-level neurophysiological state characteristics for drug evaluation in an animal model of levodopa-induced dyskinesia. *J Neurophysiol* 2016;115(3):1713–1729.
 38. Kempf F, Brucke C, Salih F, et al. Gamma activity and reactivity in human thalamic local field potentials. *Eur J Neurosci* 2009;29(5):943–953.
 39. Miocinovic S, Swann NC, de Hemptinne C, Miller A, Ostrem JL, Starr PA. Cortical gamma oscillations in isolated dystonia. *Parkinsonism Relat Disord* 2018;49:104–105.
 40. Crone NE, Miglioretti DL, Gordon B, Lesser RP. Functional mapping of human sensorimotor cortex with electrocorticographic spectral analysis. II. Event-related synchronization in the gamma band. *Brain* 1998;121(Pt 12):2301–2315.
 41. Manning JR, Jacobs J, Fried I, Kahana MJ. Broadband shifts in local field potential power spectra are correlated with single-neuron spiking in humans. *J Neurosci* 2009;29(43):13613–13620.
 42. Miller KJ, Leuthardt EC, Schalk G, et al. Spectral changes in cortical surface potentials during motor movement. *J Neurosci* 2007;27(9):2424–2432.
 43. Arlotti M, Marceglia S, Foffani G, et al. Eight-hours adaptive deep brain stimulation in patients with Parkinson disease. *Neurology* 2018;90(11):e971–e976.
 44. Little S, Tripoliti E, Beudel M, et al. Adaptive deep brain stimulation for Parkinson's disease demonstrates reduced speech side effects compared to conventional stimulation in the acute setting. *J Neurol Neurosurg Psychiatry* 2016;87(12):1388–1389.
 45. Rosa M, Arlotti M, Marceglia S, et al. Adaptive deep brain stimulation controls levodopa-induced side effects in parkinsonian patients. *Mov Disord* 2017;32(4):628–629.
 46. Velisar A, Syrkin-Nikolau J, Blumenfeld Z, et al. Dual threshold neural closed loop deep brain stimulation in Parkinson disease patients. *Brain Stimul* 2019;12(4):868–876.
 47. Little S, Beudel M, Zrinzo L, et al. Bilateral adaptive deep brain stimulation is effective in Parkinson's disease. *J Neurol Neurosurg Psychiatry* 2016;87(7):717–721.
 48. Swann NC, de Hemptinne C, Maher RB, et al. Motor system interactions in the Beta band decrease during loss of consciousness. *J Cogn Neurosci* 2016;28(1):84–95.
 49. Swann NC, de Hemptinne C, Miocinovic S, et al. Chronic multisite brain recordings from a totally implantable bidirectional neural interface: experience in 5 patients with Parkinson's disease. *J Neurosurg* 2018;128(2):605–616.
 50. Swann NC, de Hemptinne C, Thompson MC, et al. Adaptive deep brain stimulation for Parkinson's disease using motor cortex sensing. *J Neural Eng* 2018;15(4):046006.

Supporting Data

Additional Supporting Information may be found in the online version of this article at the publisher's web-site.